Ref. No.: ICF100487OR

PRESTRAINING EFFECT ON CREEP BEHAVIOUR OF Ni-BASE C263 SUPERALLOY

Yan-Hui Zhang and David M. Knowles

Department of Materials Science and Metallurgy
University of Cambridge, England CB2 3QZ

ABSTRACT

The effect of room temperature plastic deformation on the subsequent creep behaviour of C263 alloy has been studied. Creep tests were carried out at 800^{o}C and prestraining was conducted in tension up to 5.1%. Prestraining has increased primary and tertiary creep rates, but did not produce a discernible difference in the steady-state creep rate. Progressive loss of creep life and fracture ductility was found with increasing amount of prestrain. Concomitantly, the density of grain boundary cavities increased significantly, although intergranular fracture was predominant in all specimens. Cavities were found to nucleate at grain boundary carbides due to stress concentration produced by slip bands. Prolonged high temperature exposure resulted in plate-like η phase precipitation at grain boundaries. Its precipitation has been found to weaken grain boundary strength, creating cavity formation and producing microcracking.

KEYWORDS

Creep, Prestrain, Slip bands, Cavity, C263 superalloy

INTRODUCTION

It has been reported that creep performance of metals and alloys can be significantly influenced by prior plastic deformation [1-4]. Although creep strain is reduced by increased cavitation at grain boundaries, the effect of prestraining on creep strength and life is not resolved and depends on materials and testing conditions. These findings have clear technological implications since many engineering components may be strained plastically during fabrication. Another example of importance is that turbine components invariably suffer from cyclic thermal and mechanical stresses during the start-up, steady-state and shut-down operations. Plastic deformation at lower temperature can significantly influence high temperature deformation. This is especially prominent for a combustor since it suffers severe creep deformation at high temperature and plastic deformation at low temperature. In recent years, there has been an increasing interest in combustor lifing, which presents challenges not seen for turbine aerofoil and disc materials.

As part of an ongoing programme addressing combustor lifing in turbine engines, prestraining effects on creep behaviour of superalloy C263 at 800°C have been studied in this work. This alloy is widely used in non-rotating components such as combustion chambers, casing, liners, exhaust ducting and bearing housing in aeroengines.

EXPERIMENTS

The chemical composition of C263 alloy is given in Table 1. After a standard heat treatment involving solutioning at 1150°C for 2 h and ageing at 800°C for 8h, the microstructure of the material contains a mean-linear-intercept grain size of about 104 μm, an average γ′ precipitate size of ~22 nm, many annealing twins and almost continuous precipitation of $M_{23}C_6$ carbides at grain boundaries. The γ′ volume fraction was determined as ~10% using a Semper image processing program (Synoptics Ltd). $M_{23}C_6$ carbides are present along grain and twin boundaries with a finer size at the latter and are coherent with one of the neighbouring grains exhibiting the typical cube-cube relationship, i.e. $(100)_\gamma$ $//(100)_{carbide}$, $[001]_\gamma$ // $[001]_{carbide}$.

Table 1. Nominal chemical composition (wt. %) of C263 alloy.

Ni	Co	Cr	Fe	Mo	Mn	Si	Ti	Al	C
Bal.	20	20	0.7	5.8	0.6	0.4	2.15	0.45	0.06

Creep tests of non-prestrained and prestrained specimens were carried out under constant load control at 800°C at an initial stress of 160 MPa using cylindrical creep specimens with a gauge length of 28.0mm and a diameter of 5.64mm. Prestraining was carried out at room temperature at slow crosshead speed. The specimens were heated via a three-zone furnace and the temperature was controlled to ± 1.0°C over the specimen gauge length using three thermocouples and a three-term temperature controller. Strain was measured using linear variable displacement transducers capable of detecting displacement of $5x10^{-4}$ mm.

For detailed analysis of deformation and damage mechanisms, thin foils for transmission electron microscopy (TEM) observation were prepared from specimens either crept to the steady-state strain rate and then cooled down to room temperature under load, or crept to failure. TEM foils were examined in a JEOL 2000 FX electron microscope with an operating voltage of 200 kV. JEOL 820 SEM was used to characterise the microstructure of crept specimens on cross sections and fracture surfaces.

RESULTS

The creep curves of specimens prestrained and non-prestrained are shown in Fig. 1. It clearly illustrates the detrimental effect of plastic deformation on the creep life and rupture strain. This degradation in life and ductility increases consistently with increasing amount of prestrains. Comparison of these creep curves also suggests that prestraining has increased both primary creep rate and the rate of transition into tertiary creep, but not the steady-state creep rate, $\dot{\varepsilon}_S$. The average value of $\dot{\varepsilon}_S$ from three creep tests of non-prestrained specimens was $1.1x10^{-5}$, and the difference from prestrained specimens was less than

30%. It was also noticed that the proportion of life spent in steady-state creep to that in tertiary creep increased, from 0.75 for the non-prestrained specimen to 1.16 for the specimen prestrained at 5.1%.

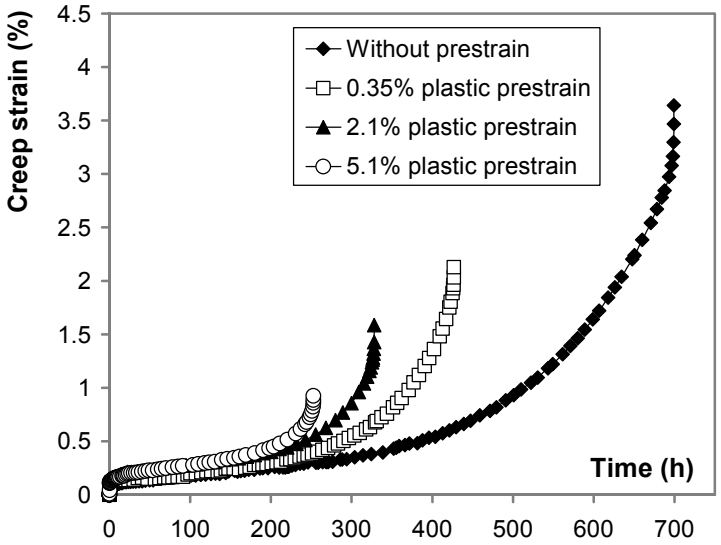

Fig. 1, Comparison of creep curves of specimens non-prestrained and prestrained, at 800^{o}C.

Microstructure analysis using TEM and SEM revealed that the limited creep strain of the material was associated with the formation of creep cavities at grain boundaries. They nucleate at the interfaces with the grain boundary carbides, see Fig. 2. Cavities formed on grain boundaries predominately normal to the loading direction, Fig. 3, and their density increased with increasing prestrains. This was suggested by both examining the cross sections and fracture surfaces of failed specimens. Although all creep fractures exhibit predominantly intergranular characteristics, there was a difference in the failure mode. For the non-prestrained specimen, failure was caused by the initiation of cracks due to cavities nucleated on the preferential sites and followed by their propagation along grain boundaries. While for the specimens with large prestrain, failure resulted mainly from the formation of cavities with higher density and more uniform distribution at grain boundaries and their subsequent coalescence. The latter can be clearly seen in Fig. 4 where cavities have almost cover the whole fracture surface of the specimen prestrained to 5.1%.

During the process of creep testings, η phase began to precipitate from grain boundaries. It exhibits a plate-like structure. These precipitates have a specific orientation relation with the γ matrix: $[011]_{\gamma}$ // $[2\bar{1}\,\bar{1}\,0]_{\eta}$, and $(11\bar{1})_{\gamma}$ // (0001). Because of the grain boundary migration driven by the energy change associated with difference in the dislocation density and chemical compositions, η phase was often found to be present along grain boundaries in the form of plates. Its nucleation was often accompanied by γ phase precipitation, forming a laminar structure, Fig. 5. Cavities were also found at such boundaries with the matrix as can be seen in this figure.

DISCUSSION

For polycrystal materials loaded under creep conditions, it has been realised that vacancies can cluster at grain boundary stress concentration sites to form cavities. These cavities accumulate to form cracks and the growth of these cracks will lead to intergranular fracture with limited creep strain. But the origin of this stress concentration is still the subject of debate. Stress concentration has been suggested to come from grain boundary sliding [5,6], slip bands [7] or grain boundary dislocation pile-up [8].

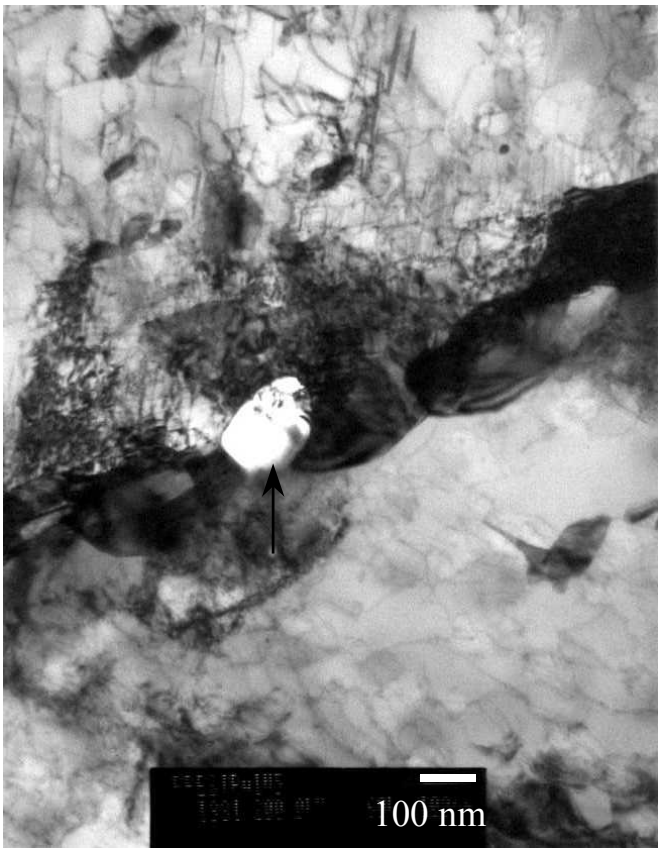

Fig. 2, TEM micrograph showing cavity nucleation (arrowed) near carbides at a grain boundary.

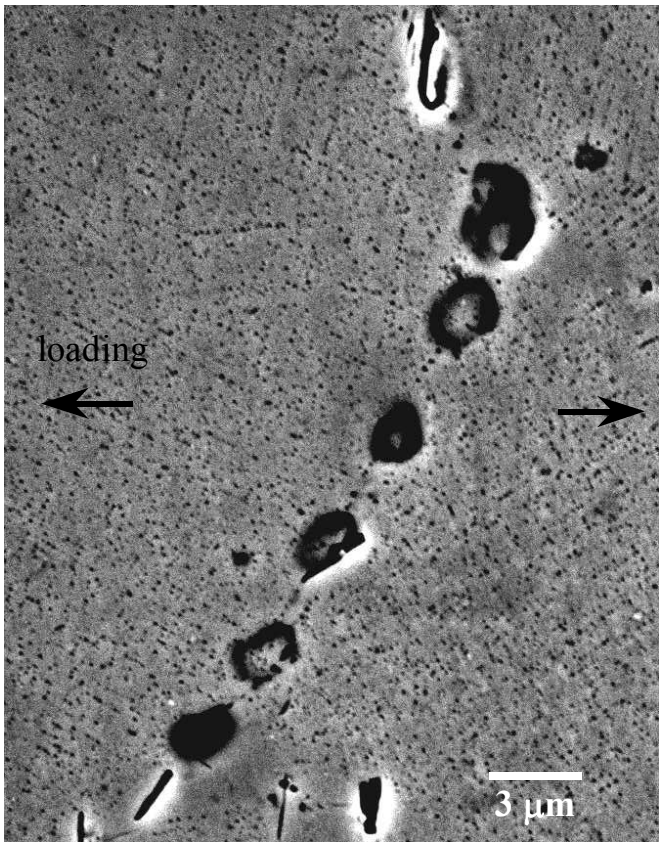

Fig. 3, Cavities nucleated extensively on grain boundary, predominantly normal to the loading direction, from the specimen prestrained to 5.1%.

A previous study on the deformation structure of the crept specimens of the alloy without prestraining has revealed that dislocation deformation was inhomogeneous and mainly located on a few slip bands during steady-state creep [9]. Stress concentration developed at the intersection of these bands with grain boundaries where carbides resides on. Cavities nucleate at the interface with the carbides due to stress concentration induced vacancy clustering. Failure was then caused by the propagation of cavity-induced cracks along grain boundaries, which resulted in a relatively extended tertiary creep stage. For the prestrained specimens, however, the current TEM observation has found that prestraining has markedly increased deformation homogeneity and produced more slip bands, see Fig. 6. This increases site density with high stress concentration at grain boundaries, resulting in a reduced incubation time for cavity formation and creating extensive cavitation on grain boundaries as can be seen in Fig. 4. Creep failure resulted from cavity linkage at grain boundaries, leading to a relatively steep tertiary creep curve.

Reports of prestraining effect on $\dot{\varepsilon}_s$ are not conclusive, as both increasing [2] and decreasing rate [3] have been observed. In this study, no discernible difference in $\dot{\varepsilon}_s$ among specimens with different amount of prestraining was detected. This might be because of the net outcome of the increased creep rate by the increased dislocation density through prestraining and the increased resistance to dislocation movement by slip band intersections. Further work will be required to identify the mechanism.

The precipitation of η phase has also been found to provide sites for cavity nucleation and microcracking [9]. Its precipitation was often accompanied by the creation of a γ′ depletion zone, which weakens the local strength of grain boundary. Furthermore, plates of this phase are regularly distributed along boundaries. Therefore, in order to improve the creep performance of the material, measures should be taken to avoid η phase precipitation at grain boundaries.

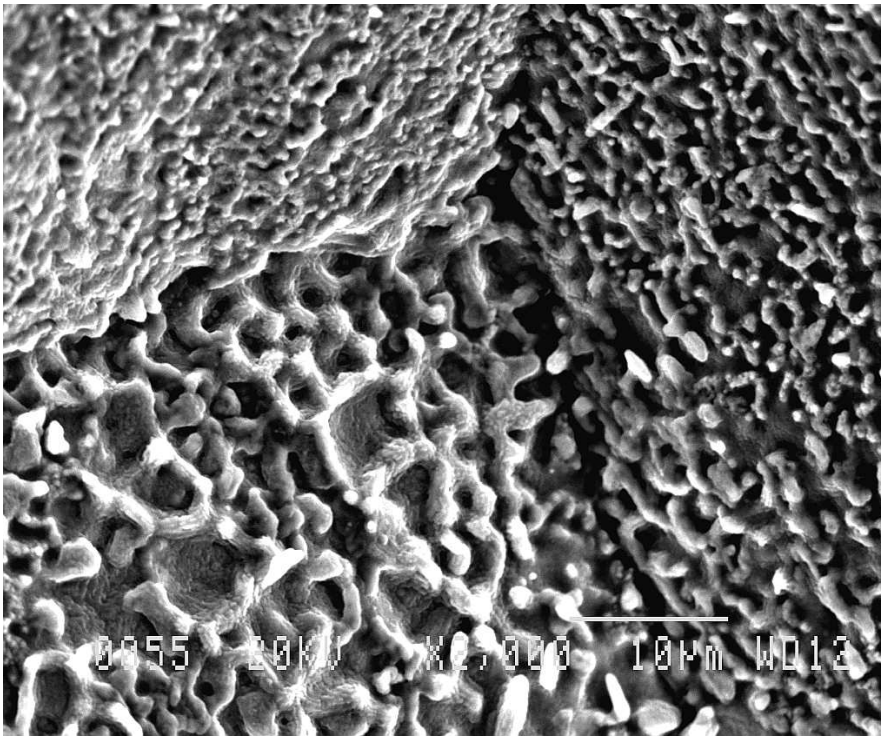

Fig. 4, SEM micrograph showing extensive cavitation on fracture surface of a crept specimen prestrained up to 5.1%.

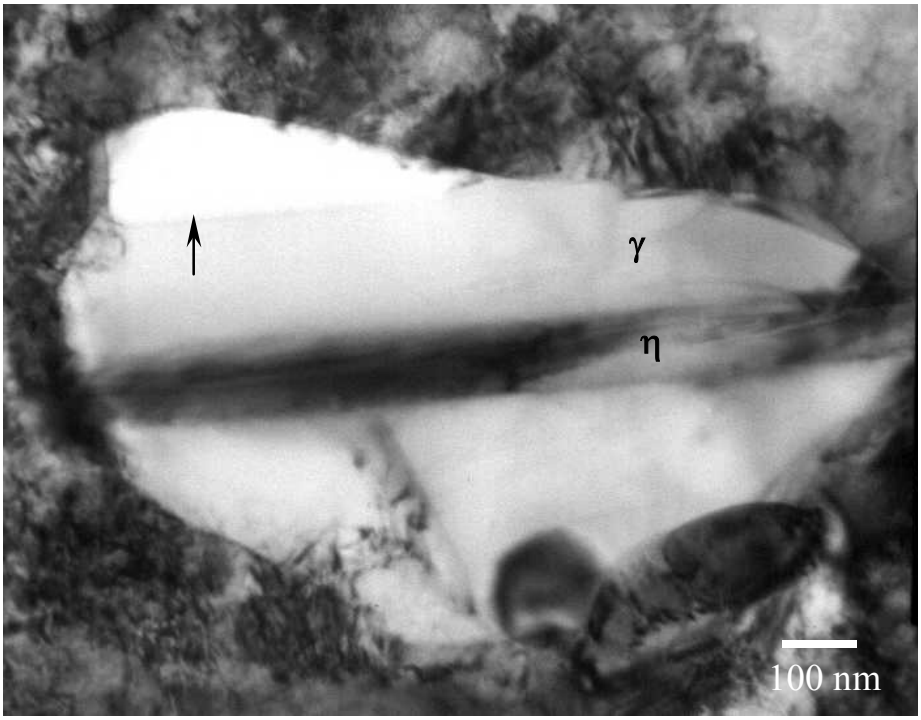

Fig. 5, Laminar structure composing of η and γ phases formed at grain boundaries. A cavity (arrowed) nucleated at the interface of γ/matrix.

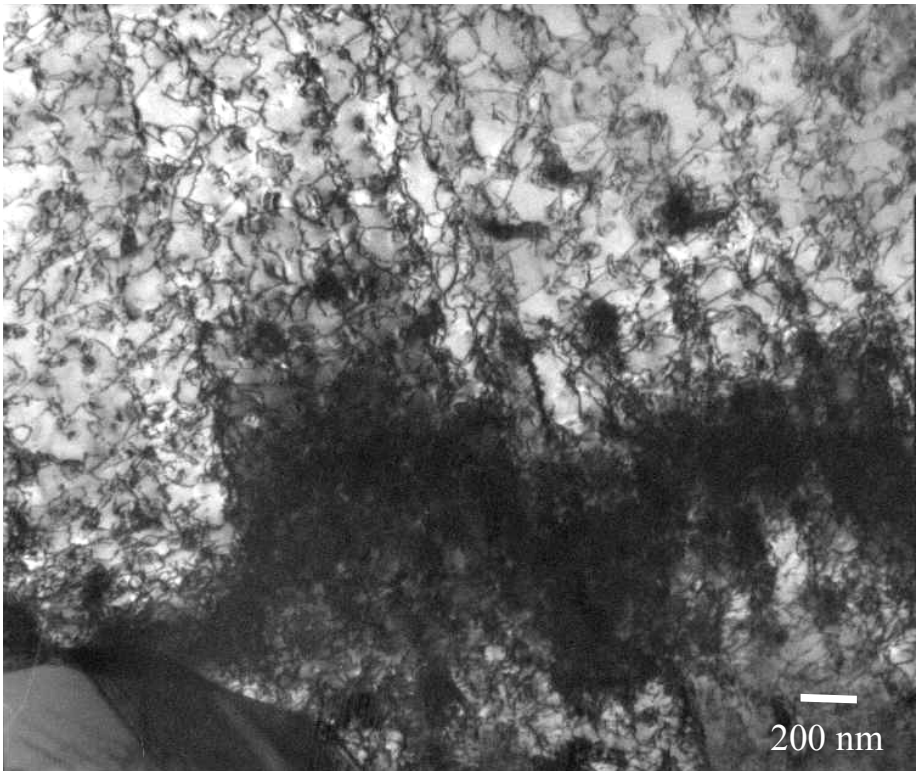

Fig. 6, TEM micrograph showing extensive slip bands structure observed in a specimen prestrained and then creep ruptured.

CONCLUSIONS

1. Creep life and rupture strain decreased with increasing prestraining.
2. Prestraining did not introduce a noticeable effect on steady-state creep rate.
3. Creep cavities nucleated near carbides at grain boundaries, which resulted in limited creep strain of the material.
4. It appears the increased cavity density with prestraining was caused by the increased stress concentration sites associated with plasticity-induced slip bands.

REFERENCES

1. Evans R.W. and Wilshire B. (1985). Creep of metals and alloys, The Institute of Metals, London.
2. Dyson B.F. and Rodgers M.J. (1974) *Metals Science*, **8**, 261.
3. Loveday M.S. and Dyson B.F. (1983) *Acta Metall*., **31**, 397.
4. Burt H., Elliot I.C. and Wilshire B. (1981) *Metals Science*, **15**, 421.
5. Raj R. and Ashby M.F. (1975) *Acta Metall*., **23**, 653.
6. Chen I.W. and Argon A.S. (1981) *Acta Metall*., **29**, 1321.
7. Dyson B.F. (1983) *Scripta Met*., **17**, 31.
8. Lim L.C. (1987) *Acta Metall*., **35**, 1663.
9. Zhang Y.H. and Knowles D.M. (2001), Proc. 9th Int. Conf. on Creep and Fracture of Engineering Materials and Structures, edited by J.D. Parker, The Institute of Materials, U.K., pp.405.